Research Papers

Experiment and Analysis of the Residual Stress for Multipass Weld Pipes by the Neutron Diffraction Method

S. H. Kim and J. H. Lee

Abstract

Multipass welds of 316L stainless steel have been widely employed to the pipes of Liquid Metal Reactors. Owing to localized heating and a subsequent rapid cooling by the welding process, residual stress arises in the weld of the pipe. In this study, the residual stresses in the 316L stainless steel pipe welds were calculated by the finite element method using the ANSYS code. Also, the residual stresses both on the surface and in the interior of the thickness were measured by the HRPD(High Resolution Powder Diffractometer) instrumented in the HANARO Reactor. The experimental data and the calculated results were compared and the characteristics of the distribution of the residual stress were discussed.

Key Words : Residual stress, 316L Stainlesss steel, Neutron diffraction, SMAW, HRPD.

1. Introduction

When the welded structure is designed and fabricated, the effects of residual stress and deformation need to be estimated. By such considerations, a stable welded structure can be maintained. The high tensile residual stress close to the weld increases the brittle fracture, the fatigue fracture and the sensibility of the stress corrosion cracking and the compressive residual stress decreases the buckling strength. A complicated problem is that the residual stress is related to the toughness as well as the size of the used materials. As the materials have a lower toughness, the residual stress can significantly decrease the fracture strength of the weld. The problem that we practically have to consider for the design of the welded structure is how to minimize the residual stress and deformation in a given environment by means of changing the thickness of the weld plate, the design of the weld joints and the welding condition and procedure. Such matters should be carried out in the first stage of design rather than the stage of fabrication.

The structural material for LMR(Liquid Metal Reactor) mainly uses austenite stainless steel 316L. The representative problem of the structural material is the creep fatigue under the high temperature sodium environment. Specially in the case of weld joints, the sodium eliminates the protection layer like the oxidized film of the material surface. This can cause material abrasions and influence the characteristics of the creep fatigue and creep fracture by the carbonization and decarbonization in the interior of the material. It is necessary to evaluate the influence of residual stress and distortion in the design and fabrication of the welded structure [1,2].

The ultrasonic diffraction technique, holl drilling technique and x-ray diffraction technique are used as the representative measurement methods of residual stress but these methods have limits for measuring the residual stress on the surface of the weld. On the other hand, a neutron is able to penetrate a few centimeters on the inside of the material so that it can be widely applied to evaluate the inside residual stress of the materials. The measurement studies of the residual stress for the multipass weld pipe were carried out by the neutron diffraction technique in the various materials [3,4].

S. H. Kim and *J. H. Lee* : Korea Atomic Energy Research Institute, Daejon, Korea
E-mail : shkim5@kaeri.re.kr

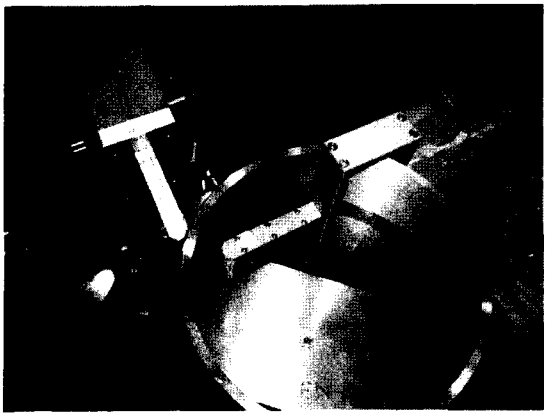

Fig. 1 Welded specimen of 316L stainless steel pipe

In this study, the experiment and analysis of the multipass weld for 316 L stainless steel pipes was carried out and the characteristics of the residual stress distribution after welding were estimated. The the HRPD(High Resolution Powder Diffractometer) instrumented in HANARO was used for the residual stress measurement. The residual stresses of the weld were calculated by the finite element method using the ANSYS code and the experimental and calculated results were compared and the characteristics of the distribution for the residual stress were discussed.

2. Specimen and experiment

2.1 Specimen

The configuration of the large pipe specimen used in this experiment is shown in Fig. 1. Two types of the small and large pipes were investigated and the data is presented in Table 1. Fig. 2 is the schematic diagram for the measurement area of residual stress in the multipass weld pipes. Two dimensional configuration and measurement points of the residual stress for the multipass welds are shown in Fig. 3. The measurement points of the residual stress are eighteen for each specimen. The welding method is SMAW(Shield Metal Arc Welding) and the welding condition is indicated in Table 2. The material of the pipes is 316L stainless steel and the filler material used in the production

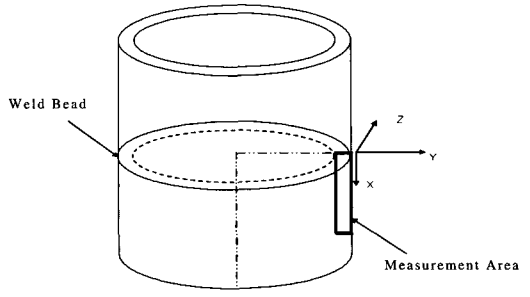

Fig. 2 Schematic diagram of multipass weld pipe

which is equivalent to E316L-16 according to the standard AWS A5.4. The filler material has higher yield strength compared to the base material [5].

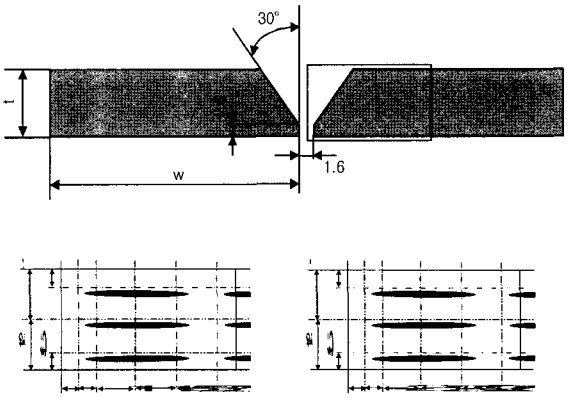

(4 inch schedule 80) (10 inch schedule 40)

Fig. 3 Configuration of the weld joints and measurement points of the experiment

Table 1 Pipe and Weld Geometries

Standard	Pipe Weld	D (mm)	t (mm)	No. of Weld Pass
ANSI 4 inch Schedule 80	SMAW	114	8.56	7
ANSI 10 inch Schedule 40	SMAW	273	9.27	8

D= outside diameter, t= nominal pipe thickness

Table 2 Welding Condition

Current (A)	Voltage (V)	Welding Speed (mm/min)
120	30	350

2.2 Principles of the neutron diffraction technique

When a beam of neutrons of wavelength λ is incident on a crystalline material as shown in Fig. 4, a diffraction pattern with sharp maxima is produced. The angular positions of the maxima for a family of crystallographic planes of separation d are given by te Bragg equation

$$2d \sin\theta = n\lambda \quad (1)$$

where n is an integer and 2θ is the diffraction angle. Measurements can be made with a continuous monochromatic or a pulsed polychromatic beam of neutrons. For a monochromatic beam of constant wavelength any change in lattice spacing Δd will cause a corresponding shift $\Delta\theta$ in the angular position of the Bragg reflection so that the lattice strain in the direction of the scattering vector Q is given by

$$\varepsilon = \frac{\Delta d}{d} = -\Delta\theta \cot\theta \quad (2)$$

To calculate absolute values of strain, the unstressed lattice spacing d_o must be known. Also, in general, to define the strain tensor at a point completely, measurements in six orientations are required. However, when the principal directions are known, three will suffice. When these coincide with the coordinate directions x, y and z, the principal stresses are given by

$$\sigma_x = \frac{E}{(1+\nu)(1-2\nu)}[(1-\nu)\varepsilon_x + \nu(\varepsilon_y + \varepsilon_z)] \quad (3)$$

with corresponding expressions for σ_y and σ_z. In this equation, E is the elastic modulus and ν Poission's ratio [6].

2.3 Experiment procedure

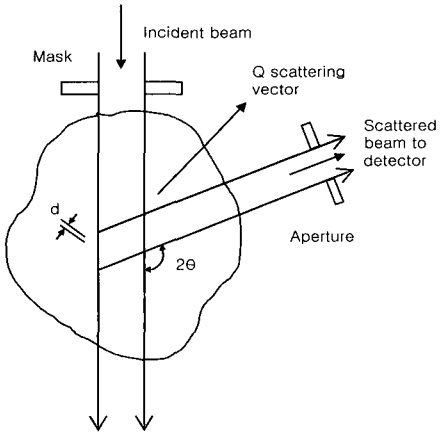

Fig. 4 Principles of neutron diffraction

For measuring the residual stress of the welded pipe specimen, HRPD in Fig. 5 was used. The experiment procedure using neutron diffraction consists of three steps. First is the initial stage that decide the position of the equipments and the size of the slit, and measures the wavelength of the neutron beam. Second is the measuring of the distance between the lattices do for the specimen in a condition of zero stress and this becomes the standard value for the measurement of the residual stress. Finally, after fixing the welded specimen at the sample stage, we measure the distance(d) between the diffraction measurement volumes from each measurement direction.

Fig. 5 High Resolution Powder Diffractometer

Fig. 6 is the conceptual diagram of the experiment equipment. The center axis is decided by fixing the

incident beam positioned at the right side and adjusting the X-Y direction translator under the specimen holder and the detector at the left side in the figure. In order to measure the strain components of the three rectangular coordinate directions (normal, transverse, longitudinal directions), each welded specimen is positioned.

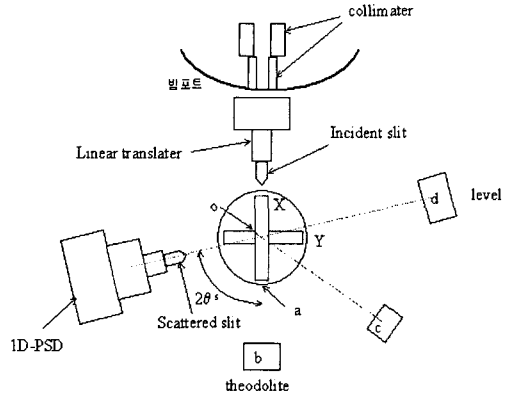

Fig. 6 Schematic diagram of experimental apparatus

2.4 Discussion of the experiment results

The overmatched filler material was used for the weld of 316L stainless steel pipes chosen in the experiment. The filler material used has about a double yield strength from that of the base material at room temperature. The experimental results of the hoop residual stress for the small and large pipes is presented in Fig. 7 and Fig. 8. The maximum hoop residual stress is about 450 MPa at the weld centerline for both types of specimens. This value is similar to the yield stress of the applied filler material and it seems that the maximum hoop residual stress has a close relation with the yield stress of the filler material. The maximum axial residual stress ,as shown in Fig. 9 and Fig. 10, is 306MPa for the small pipe and 210MPa in large pipe and these values are far smaller in comparison with the maximum hoop residual stress. Comparing the distribution of the residual stresses between the outer and inner surface of the pipes, the hoop residual stress of the weld centerline has larger value at the inner surface for the large pipe but shows a larger value at the outer surface for the small pipe. The axial residual stress of the small and large pipes is presented in Fig. 11. The entire axial residual stresses were larger for the small pipe than for the large pipe [7,8].

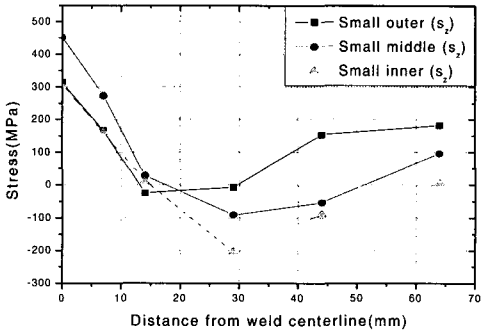

Fig. 7 Distribution of the hoop residual stresses from the experimental data(small/4 inch dia.)

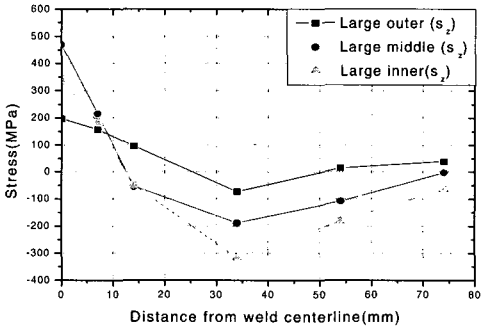

Fig. 8 Distribution of the hoop residual stresses from the experimental data(large/10 inch dia.)

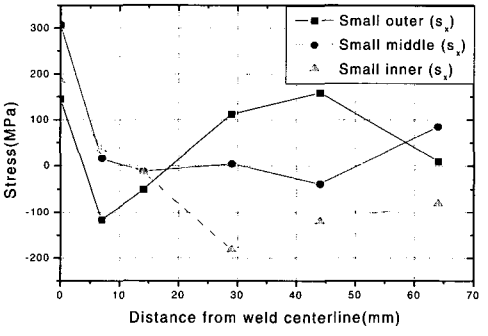

Fig. 9 Distribution of the axial residual stresses from the experimental data(small/4 inch dia.)

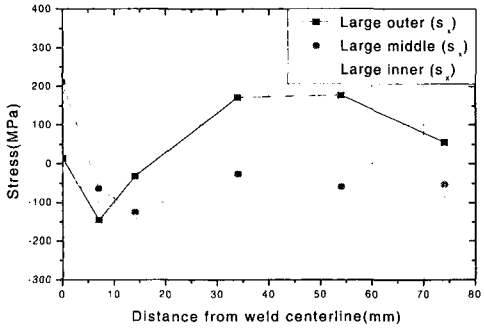

Fig. 10 Distribution of the axial residual stresses from the experimental data(large/10 inch dia.)

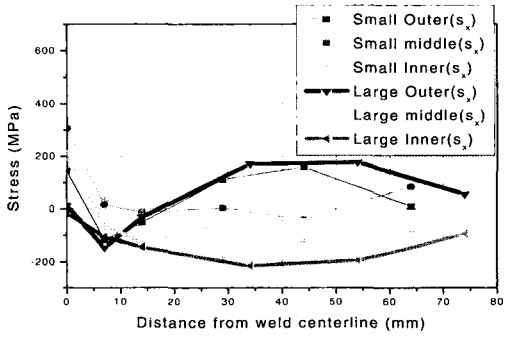

Fig.11 Distribution of the axial residual stresses from the experimental data

3. Analysis of multipass weld of the pipes

3.1 Boundary condition

We used the two-dimensional axisymmetric model for the cross sectional area of the welded pipes, assuming the insulation in the left side of the model. Heat input was modeled by adding the uniform temperature above the melting point as a thermal load to the element equivalent to the molten metal. Also, the natural convection coefficient used was 1.95W/㎡ at the outer surface and a half of the outer surface to the inner surface and the radiation effect was ignored [9].

Fig. 12 is the configuration of finite element model for the small pipe. The boundary conditions of model has the plain strain with the constraint on the x-directional displacement of the left symmetric axis and the lowest right node is simply supported in the y-direction.

Fig.12 Finite element model of analysis area

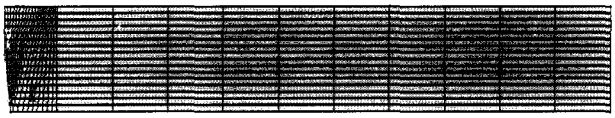

3.2 Analysis model

The thermal-structural analysis for the multipass welds was performed by the sequential weak coupling method. The coupled field element PLANE 13 was used so that the transient temperature distribution and the corresponding static thermal stresses were determined at the same time. Element Birth and Death Option of the ANSYS Code was used. The weld bead was applied by making the bead elements alive at the liquid temperature. As the bead cools, the structural material properties increase in strength and the thermal stresses develop the plastic strains.

The thermal properties of the base and weld material are shown in Table 3 and the mechanical properties are shown in Table 4. The Von Mises yield criterion was used to define the onset of yielding. Once yielding has occurred an associated flow rule is used to calculate the incremental plastic strains. In this study a rate independent plasticity model with a kinematic hardening assumption has been adopted to characterize the material behavior during the welding. The stress at the melting temperature is 0.8% of the yield stress at room temperature. Even though the weld area has seven and eight pass welds, the weld material was modeled by four lumped passes and each pass was serially added to the weld area from a lower part [10].

Table 3 Thermal Properties of 316 L Stainless Steel

T(°C)	C_p(J/kg °C)	k(W/m °C)
40	450	15
400	570	20
800	620	25
1200	700	31
1390	730	33
1600	730	90

C_p= Specific Heat, k= Thermal Conductivity

Table 4 Mechanical Properties of 316 L Stainless Steel and Weld Metal

T (°C)	E (GPa)	Sy (MPa) Base	Sy (MPa) Weld	E_T (MPa)	ν	α (1/ °C)
40	210	230	460	2800	0.26	19×10^{-6}
400	168	139	278	2370	0.32	19×10^{-6}
800	133	80	160	1900	0.25	19×10^{-6}
1200	55	22	22	600	0.24	19×10^{-6}
1390	10	2	2	100	0.24	19×10^{-6}
1600	10	2	2	100	0.24	19×10^{-6}

ν = Poissions Ratio, α = Linear Thermal Expansion Coefficient
E= Elastic Modulus, s_y= Yield Stress, E_T=Tangent Modulus

3.3 Analysis results

3.3.1 Distribution of the temperature and residual stress

The temperature distribution of the weld after the first weld pass is shown in Fig. 13 (1 pass). After some time interval, the temperature of the weld was sufficiently cooled and then the rest of the weld pass was serially added from the lower part to upper part. The calculated temperature distribution of the weld after 10 sec from the moment each weld pass was added is shown in Fig. 13(2,3,4 pass). The distribution of the hoop residual stress around the weld is developed with time as follows. After the first pass is processed the maximum tensile hoop stress is generated at the bottom of the weld. After the second pass, the maximum value of the hoop stress moves up to the region of the second pass. However, the change of the hoop residual stress after the second pass is not so large. The maximum tensile hoop stress after each pass moves from the previous lower pass to the upper pass and the stress area increases. After the final pass the maximum stress is situated at the top of the weld [11].

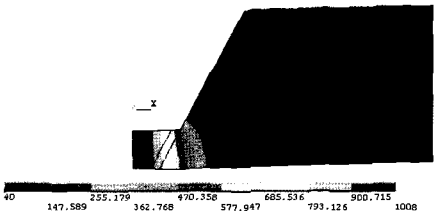

(a) 1 pass

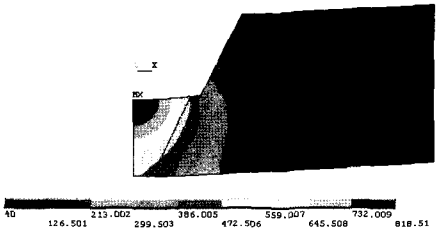

(b) 2 pass

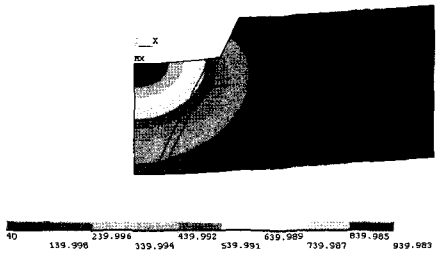

(c) 3 pass

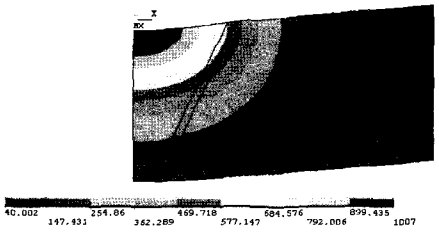

(d) 4 pass

Fig . 13 Temperature distribution of the weld after each weld pass

3.3.2 Distribution of the residual stress for a small pipe

The stress that is parallel to the working direction of the weld bead is the hoop residual stress and is indicated by S_z and the axial residual stress is indicated in S_x. The ratio of the thickness to the diameter (t/d) of the small pipe(4inch schedule 80) is 0.075. The distribution of the residual stress of the outer surface according to the distance to the x-direction from the weld centerline is shown in Fig. 14. The hoop residual stress measured on the weld centerline is 303MPa and it agrees well with the analysis value. According to the analysis results, the high tensile stress is distributed in the area between the weld centerline and HAZ and the maximum tensile stress occurs at a point in that area. Outside that area the residual stress decrease rapidly and is transformed into a compressive stress as the distance from the weld centerline increases. With reference to Fig. 15 and Fig. 16 for the stress distribution in the middle and inner surface of the pipe,

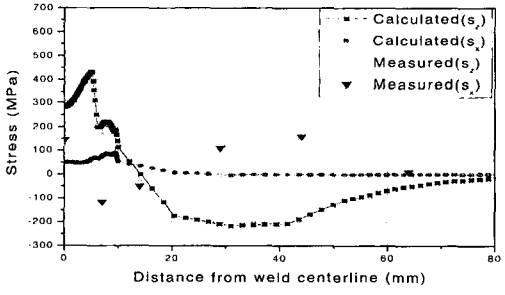

Fig. 14 Hoop and axial residual stresses on outer surface (4 inch dia.)

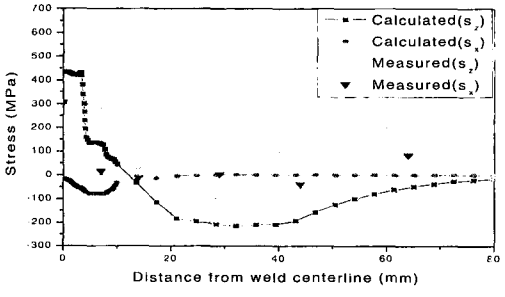

Fig. 16 Hoop and axial residual stresses on middle surface (4 inch dia.)

the maximum hoop residual stress was generated at the weld centerline for both cases. The maximum hoop residual stress of 451MPa was generated at the middle surface of the pipe. The lowest hoop residual stress in the weld centerline was generated at the inner surface.

The axial residual stress is smaller than the hoop residual stress in the weld but larger in the base material outside HAZ.

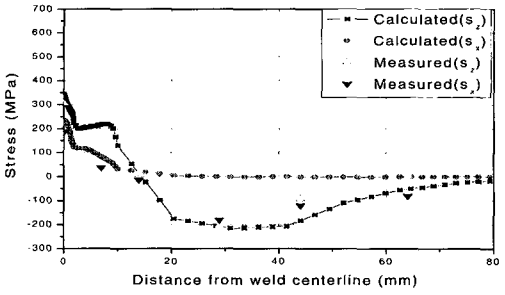

Fig. 17 Hoop and axial residual stresses on inner surface (4 inch dia.)

3.3.3 Distribution of the residual stress for large pipe

The ratio of the thickness to the diameter (t/d) of the large pipe(10 inch schedule 40) is 0.034 and it has a small thickness in comparison with the large diameter of the pipe. Because of the smaller temperature difference between the inner and outer surfaces in such a type of pipes, the thermal stress is reduced. The distribution of the residual stress at the outer surface with the distance along the x-direction from the weld centerline is presented in Fig. 17. The value of the residual stress measured at the weld centerline

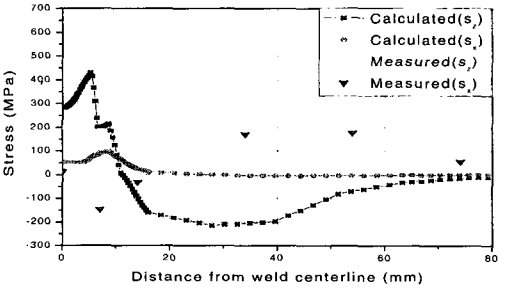

Fig. 17 Hoop and axial residual stresses on outer surface (10 inch dia.)

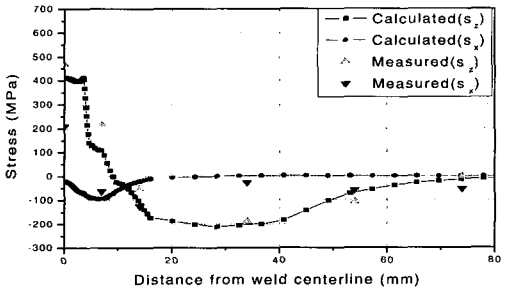

Fig.18 Hoop and axial residual stresses on middle surface (10 inch dia.)

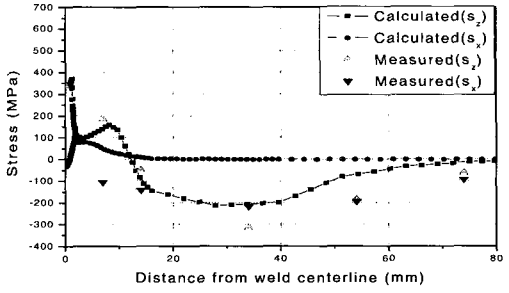

Fig. 19 Hoop and axial residual stresses on inner surface(10 inch dia.)

was smaller than the small pipe and the analysis value was calculated to be larger than the experiment value.

The distribution of the hoop residual stress at the middle and the inner surface of the pipe is presented in Fig. 18 and Fig. 19. The results of the experiment and analysis have some difference quantitatively but a good agreement qualitatively and it has a similar tendency with the results of the small pipe[12].

4. Conclusion

The residual stresses both on the surface and in the interior of the thickness were measured in the small(t/d=0.075) and large pipe specimens (t/d=0.034) with the multipass welds of the 316L stainless by using the neutron diffraction method. The experiment results were compared to the analysis results by the finite element method and the following results were obtained.

1. The maximum hoop and axial residual stress are created at the middle surface of the two pipe specimens. The maximum value both for the large and small pipe specimens is about 450MPa and it is similar to the yield stress of the filler material. It seems that the maximum hoop residual stress has a close relation with the the yield stress of the filler material. The maximum axial residual stress was 306MPa for small pipe and 210MPa for the large pipe and these values are much smaller in comparison with the maximum hoop residual stress.

2. The hoop residual stress of the weld centerline had a larger value at the inner surface for the large pipe, but showed a larger value at the outer surface for the small pipe.

3. In comparison with the small and large pipes, the entire axial residual stresses were larger for the small pipe than for the large pipe.

4. In the analysis results of the hoop residual stress, the maximum tensile stress was created in the weld close to HAZ at the outer surface of the pipe and in the weld centerline at the middle and inner surface of the pipe. The analysis results of the hoop residual stress are in good agreement with the experimental results but those of the axial residual stress were evaluated to be relatively small in the weld.

Acknowledgements

This work was performed under the long term nuclear R&D program sponsored by the Ministry of Science and Technology of Korea.

References

1. J. C. Suarez, L. Murakawa, and Y. Ueda : Effect of welding residual stress on fracture toughness testing, *Trans. JWRI*, Vol. 26, No. 1 (1997), pp. 28-35
2. T. Chapman, H. Offer, W. Sanders, and G. Rusack : Reduced stress welding process for nuclear plant

piping, *Nuclear Engineering and Design*, Vol. 170, (1997), pp. 81-88
3. R. A. Owen, R. V. Preston, P. J. Withers, H. R. Shercliff, and P. J. Webster : Neutron and synchrotron measurements of residual strain in TIG welded aluminium alloy 2024, *Material Science and Engineering*, Vol. A346, (2003), pp. 159-167
4. M. J. Park, D. Y. Jang, and H. D. Choi : Residual stress measurement on welded specimen by neutron diffraction, *Journal of KWS*, Vol. 20, No. 2 (2002), pp. 168-176 (in Korean)
5. P. Dong and J. Zhang : Residual stresses in strength-mismatched welds and implications on fracture behavior, *Engineering Fracture Mechanics*, Vol. 64, (1999), pp. 485-505
6. G. A. Webster and R. C. Wimpory : Non-destructive measurement of residual stress by neutron diffraction, *Material Processing Technology*, Vol. 117, (2001), pp. 395-399
7. B. Brickstad and B. L. Josefson : A parametic study of residual stress in multi-pass butt-welded stainless steel pipes, *International Journal of Pressure Vessels and Piping*, Vol. 75, (1998), pp. 11-25
8. F. Faure and R. H. Leggatt : Residual stresses in austenitic stainless steel primary coolant pipes and welds of pressurized water reactors, *International Journal of Pressure Vessels and Piping*, Vol. 65, (1996), pp. 265-275
9. H. Murakawa : Theoretical prediction of residual stress in welded structures, *Welding International*, Vol. 11, No. 8 (1997), pp. 2-7
10. C. K. Leung and R. J. Pick : Finite element analysis of multipass welds, *WRC Bulletine*, Vol. 356, (1990), pp. 11-33
11. J. B. Roelens, F. Maltrud, and J. Lu : Determination of residual stresses in submerged arc multi-pass welds by means of numerical simulation and comparison with experimental measurements, *Welding in the World*, Vol. 33, No. 3 (1994), pp. 36-43
12. T. L. Teng and P. H. Chang : A study of residual stresses in multi-pass girth-butt welded pipes, *International Journal of Pressure Vessels and Piping*, Vol. 74, (1997), pp. 59-70